SHIELDING PROPERTIES OF FLY ASH BASED GEOPOLYMER USING BARIUM SULPHATE FOR DIAGNOSTIC RADIOLOGY

SABRI MANSUR HIMEEDH SHALBI

UNIVERSITI SAINS MALAYSIA

2018

DEDICATION

I would like to dedicate this work to the soul of my father Mansur Alshalbi who passed away while I was doing my research. I also dedicate this work to my mother Maso'uda Hussin Alshalbi whose prayers have given me the strengths to complete this work. I am profoundly grateful to my parents.

I want to thank my wife Fatheia Hussin and my lovely kids Mohammed, Rawasi, Ekhlas, and Isra. I do not have appropriate words to weight their encouragement, cooperation, patience, and understanding to achieve my goals to finish my work.

SHIELDING PROPERTIES OF FLY ASH BASED GEOPOLYMER USING BARIUM SULPHATE FOR DIAGNOSTIC RADIOLOGY

by

SABRI MANSUR HIMEEDH SHALBI

Thesis submitted in fulfillment of the requirements
for the degree of
Doctor of Philosophy

February 2018

ACKNOWLEDGEMENT

The submission of this thesis gives me an opportunity to express all praises to Allah, the almighty, merciful and passionate, for granting me the strengths to complete this thesis.

I highly show my regards to my main supervisor Prof. Dr. Mohamad Suhaimi Jaafar for his great support, guidance in completion of my research work and patiently correcting my writing. I attribute the level of my PhD degree to his great help and encouragement. One simply could not wish for a better or friendlier supervisor. I would like to express my great thanks to my co-supervisor, Dr. Naser Mohammed Ahmed, for his excellent guidance, caring, patience, and providing me with an excellent atmosphere for doing my research. He is really very expert in his field and has directed me through various situations, allowing me to reach this accomplishment.

Special thanks go to the supporting staff of the laboratories in School of Physics, and School of Civil Engineering who helped me in many different ways to conduct the experiments in a specific manner. I would like to thank the technicians at the School of Physics, USM, Mr. Mohd Rizal Mohamad Rodin, Mr. Hazhar Hassan and Mr. Mohamed Mustaqim Ab Bakar for their help during my work in the laboratory. I thank also Universiti Sains Malaysia, which granted me the chance to pursue my PhD at the School of Physics where I have had ample access to various facilities. I offer my regards and blessings to all of those who supported me in any respect during the completion of the research, as well as expressing my apology to that I could not mention personally one by one.

Finally, A special word of thank goes to my friends Dr. Amer Aljarrah, Dr. Mostafa Jomaah, Dr. Abdallah Taher , Dr. Motahher Abdallah, Dr. Ali Abu Arrah and Dr. Bakr M. and my colleague Nor Ain Rabaiee, Othman Elbasir for their support and help.

TABLE OF CONTENTS

LIST OF TABLES

Page

LIST OF FIGURES

Page

LIST OF ABBREVIATIONS

ALARA	As low as reasonably achievable
^{241}Am	Americium source
ASTM	American society of testing and materials
EDX	Energy dispersive X-ray spectrometer
eV	Electron volt
FA	Fly ash
FAGP	Fly ash geopolymer
FESEM	Field emission scanning electron microscopy
GPCC	Geopolymers concrete composite
IAEA	International atomic energy agency
keV	Kilo electron volt
kV	Kilo volt
kVp	Peak kilovoltage
LE-Ge	Low energy germanium
m/v	Mass per volume
mAs	Milliampere second
MPa	Megapascal
MPV	Mean pixel value
OPC	Ordinary Portland cement
OD	Optical density
R^2	Linear regression coefficient
ROI	Region of interest
SG	Specific gravity

SSD	Saturated –surface- dry
Ti	Titanium
XCOM	X-ray computed
XRF	X-ray fluorescence
XR-QA2	Gafchromic film

LIST OF SYMBOLS

%	Percentage
γ	Gamma
μ	Linear attenuation coefficient
P	Density
μ	Linear attenuation coefficient
ρ	Density
μ/ρ	Mass attenuation coefficient
Ag	Silver
Al	Aluminium
Al_2O_3	Aluminium oxide
Ba	Barium
$BaSO_4$	Barium sulphate
C	Carbon
Ca	Calcium
CaO	Calcium oxide
cm	Centimetre
cm^{-1}	Inverse centimetre
Cm^2/g	Square centimetre / gram
℃	Celsius degree temperature
Cm^3	Cubic centimetre
CO_2	Carbon dioxide
Eq	Equation
Fe	Iron
g/cm^3	Gram /centimetre cube
H_2O	Water

Gy	Gray
I	Exit intensity of photon
I_o	Initial intensity of photon
K	Potassium
Kg	Kilogram
m	Mass
M	Molarity
m_{air}	Air of mass
Mg	Magnesium
mm	Millimetre
Mo	Molybdenum
Ms	Silica modulus
Na_2SiO_3	Sodium silicate
µ Gy	Micro gray
Na	Sodium
NaOH	Sodium hidroxide
Np	Niobium
nC	Nano-coulomb
O	Oxygen
Pd	Palladium
Q	Charge
S	Sulfur
Si	Silicon
Sn	Tin
t	Thickness
Ti	Titanium
ν	Volume

Z	Atomic number
Z_{eff}	Effective atomic number

SIFAT-SIFAT PERISAI GEOPOLIMER BERASASKAN ABU TERBANG MENGGUNAKAN BARIUM SULFAT UNTUK DIAGNOSTIK RADIOLOGI

ABSTRAK

Kajian ini dijalankan bagi mengkaji sifat-sifat abu terbang geopolimer (FAGP) untuk digunakan sebagai alternatif bahan semen mortar (OPC) sebagai bahan perisai dengan menambahkan barium sulfat ($BaSO_4$) sebagai bahan tambahan. Fabrikasi FAGP melibatkan pembubaran bahan aluminosilikat dalam larutan yang sangat alkalin dan kombinasi selanjutnya dengan pasir. Ciri-ciri perisaian FAGP dipertingkatkan dengan penambahan $BaSO_4$. FAGP dikeringkan dalam ketuhar selama satu hari pada 60-70 ℃, dan kemudian disejukkan pada suhu bilik selama 28 hari. FAGP yang difabrikasi telah dilakukan analisis komposisi keunsuran menggunakan spektroskopi sinar-X penyebaran tenaga (EDX) untuk menghitung Z_{eff} yang seterusnya memberi petunjuk kepada keupayaan FAGP sebagai perisai. Untuk menunjukkan wujudnya atenuasi apabila menggunakan FAGP sebagai perisai, μ/ρ dihitung menggunakan program XCOM untuk semua sampel. Nilai μ/ρ OPC, FAGP, FAGP dengan 5%, 10%, dan 15% $BaSO_4$ diukur pada tenaga 16.61, 17.47, 21.17, 22.16 dan 25.27 keV dengan menggunakan pendarfluor sinar-X (XRF). Geometri alur sempit digunakan untuk mengukur dos peancaran, μ/ρ dan peratusan atenuasi sampel menggunakan tenaga 59.54 keV. Untuk mendapatkan ketebalan FAGP yang setara dengan atenuasi ketebalan 1 mm plumbum, sinar-X dengan 80, 100, dan 120 kVp digunakan untuk membandingkan ketebalan FAGP + 15% $BaSO_4$ dengan ketebalan plumbum memandangkan kapasiti perisaian optimum dicapai dengan ketebalan 5 cm $BaSO_4$ 15% dan 1 mm plumbum. Berasaskan kepada keputusan

optimum yang diperoleh, rekabentuk kotak perisai difabrikasi dengan ketebalan 5 cm dan 15% $BaSO_4$ ditambahkan kepada FAGP. Prestasi kotak perisaian telah dinilai dengan mengira μ/ρ melalui dua cara pengiraan, iaitu, filem dosimetri Gafchromic XR-QA2 dan pengiraan kebuk ion, menggunakan menggunakan 80, 100 dan 120 kVp sinar-X diagnostik. Dalam kajian ini, jelas bahawa FAGP adalah bahan yang sesuai untuk digunakan sebagai bahan perisaian sinaran. Keputusan menunjukkan bahawa FAGP dengan penambahan 15% $BaSO_4$ adalah bahan atenuasi yang baik untuk sinar-X diagnostik bertenaga rendah.

SHIELDING PROPERTIES OF FLY ASH BASED GEOPOLYMER USING BARIUM SULPHATE FOR DIAGNOSTIC RADIOLOGY

ABSTRACT

This work was conducted to study the properties of fly ash geopolymer (FAGP) in order to use as an alternative cement mortar (OPC) material as shielding material by adding barium sulphate ($BaSO_4$) as an additional material. The fabrication of the FAGP involved the dissolution of aluminosilicate material in a highly alkaline solution and subsequent combination with sand. The shielding properties of FAGP were enhanced with the addition of $BaSO_4$. The FAGP was dried in an oven for one day at 60 - 70 ℃, and then cooled at room temperature for 28 days. The fabricated FAGP was subjected to elemental composition analysis using energy dispersive X-ray spectroscopy (EDX) to calculate the Z_{eff} which in turn hints to the ability of FAGP in shielding. To indicate the presence of attenuation when using the FAGP in shielding, the μ/ρ was calculated by XCOM program for all the samples. The μ/ρ of OPC, FAGP, FAGP with 5%, 10%, and 15% $BaSO_4$ was measured at 16.61, 17.47, 21.17, 22.16 and 25.27 keV energies using X-ray fluorescence (XRF). Narrow beam geometry was used to measure transmission does, the μ/ρ and attenuation percentages of the samples using the energy of 59.54 keV. To obtaining the thickness of FAGP which equivalent in attenuation to the 1mm thickness of lead, X-ray with 80, 100, and 120 kVp was used to compare the FAGP + 15% $BaSO_4$ thicknesses with the thicknesses of lead, as the optimal shielding capacity was achieved with 5 cm thick FAGP with 15% $BaSO_4$ and 1 mm thick lead. Based on the optimum results obtained, the design shielding box was fabricated with

5 cm thickness and 15% $BaSO_4$ added to FAGP. The performance of the shielding box was evaluated by calculating the μ/ρ by two ways, that is, Gafchromic XR-QA2 dosimetry film and ion chamber calculation, using 80, 100 and 120 kVp diagnostic X-ray. In this study, it is clear that the FAGP is a promising material to be used in shielding materials. The results show that the FAGP with addition of 15% $BaSO_4$ is a good attenuation material for diagnostic X-ray of low energies.

CHAPTER 1: INTRODUCTION

1.1 Background to study

Fly ash geopolymer (FAGP) is a material producing by burning the coal in the electricity power station. The abundant of fly ash (FA) worldwide creates an opportunity to utilise this by-product of burning coal, as a substitute for Ordinary Portland Cement (OPC) to manufacture concrete. When used as a partial replacement of OPC. The development and application of high volume FA concrete, which enabled the replacement of OPC up to 60% by mass (Malhotra, 2002), is a significant development.

FA is a source material for geopolymer binders that is readily obtainable, but its use to date is limited. More specifically, the global coal ash production estimation exceeded 390 million tonnes annually; but its use fell below 15% (Malhotra, 1999). OPC is normally used in building walls and roofs but it is not environmentally friendly as FAGP. The FAGP has improved adhesion properties and is denser than OPC. FAGP were to limit the amount of energy required to manufacture OPC. Moreover, it has also reduced the emission of harmful gases, produced in OPC factories to a significant extent (Chindaprasirt et al., 2007, Malhotra, 2002).

Concrete is one of the main materials used in shielding. There are some disadvantages in its use as shielding materials. Some of these problems are substantial inconsistency in its composition and its moisture content. The disparity in composition brings about ambiguity in calculations for shield design predictions of the radiation distribution and attenuation, while water content lowers both the density and structural strength of concrete. However, the loss of water is the major drawback

of concrete because concrete becomes hot due to moisture loss by absorption of radiation energy (Manohara et al., 2009). In addition to the concrete that contains amounts of cement for approximately between 6% and 7% of all CO_2 emission in the atmosphere. In turn, CO_2 contributes almost 65% of global warming (Rashad, 2014). Researcher Stankovic et al. focused on the influence of the OPC on the radiation protection ability of concrete. In order to compare between the transmission factors, absorbed energy and mass attenuation coefficients of OPC. Results of the study proved that barium can considerably improve the radiation protection ability of OPC (Stanković et al., 2010).

OPC may be effective in shielding for radiation protection after the addition of barium $BaSO_4$, however, it is an expensive material compared to a waste material, FAGP. FAGP is less expensive and less emission of CO_2 to the environment. On the other hand, using OPC in X-ray room wall construction has some disadvantages such as the OPC is consequently one of the largest global sources of combustion and chemical process related carbon dioxide emissions, accounting for 5% of global CO_2 production or approximately 1.5 tons per year (Kotwal et al., 2015). Thus, a small reduction of Portland cement production could result in significant environmental benefits in terms of CO_2 emission.

The key objective of radiation protection is to shield human and environment from the damaging effect of ionizing radiation without overly limiting the valuable applications of such exposures such as radiation medical uses (Luykx and Frissel, 2012). There is a growing demand for radiation technologies, specifically radioactive isotopes and accelerators in several fields of science. However, these technologies are compelled to be used with extreme caution and only after putting in place

effective protective shields. Taking this into account, it is vital to study the level of radiation people are exposed to in their homes. Thus, the two key general points that should be taken into consideration in the field of building construction are resistance to earthquake expressed as strength of the building and resistance to radiation expressed as γ-ray attenuation (Akkurt et al., 2005).

The importance of γ-ray is based on in its ability to easily penetrate into matter since it is uncharged and has no mass, and hence challenging to shield. Nonetheless, the interaction of γ-rays depends on the incident photon energy. The penetration and diffusion of the radiation through a medium is dependent on linear attenuation coefficients (μ), which is defined as the probability of a radiation interacting with a material per unit path length. The magnitude of μ depends on incident photon energy, atomic number and density of the shielding materials. Based on the dependence of μ on density (ρ), it is defined as mass attenuation coefficients (μ/ρ), which is the linear attenuation coefficient per unit mass of the material (Medhat, 2009).

The precise values of (μ/ρ) for X-ray in several materials is vital in the fields of nuclear and radiation physics, radiation dosimetry, in addition to biological, medical, agricultural and industrial applications. There are a number of experimental and theoretical studies on (μ/ρ) (Han et al., 2009). For example, calculated (μ) of OPC mixed with silica fume, blast furnace slag and natural zeolite over the range of 1–2000 keV (Türkmen et al., 2008). Khalid and others in 2015 also calculated (μ/ρ) of barium sulphate with cement used in preference to concrete as a shield against radiation (Khalid et al., 2015). Measured γ-ray attenuation coefficients of limestone, bricks and concrete in Jordan. (Salinas et al., 2006). Likewise, calculated the density

and (μ/ρ) of several building materials usually used in Brazil (Akkurt et al., 2004). Also calculated the attenuation coefficients of barite, marble and limra in Turkey (Akkurt et al., 2004) measured (μ/ρ) for soil samples and building materials in Bangladesh.(Meckbach et al., 1987).

Radiation shielding is based on the principle of attenuation, which is the ability to reduce radiation penetrating through a barrier material by blocking or bouncing off particles. However, the effects and degree of radiation penetration vary in relation to the type of radiation involved. In last decades, extensive studies were carried out to improve the radiation shielding efficiency of several materials such as ordinary concrete, heavy concrete, lead, steel, polyethylene, paraffin and wood (McCaffrey et al., 2007a, Stam and Pillay, 2008). These materials are normally used to shield harmful effects of radiation. Concrete has several advantages over other materials. Some of these advantages are its provision of effective X-ray shielding, high structural strength and cost effectiveness. Similarly, lead has a high atomic number (Z) that makes it to be used for effective shielding of the X-ray, although its toxicity feature is a major concern, particularly when occupational exposure is considered. In contrast to concrete materials, steel is expensive but non-toxic. Moreover, steel is more effective than concrete as an X and γ-rays shielding material, but it is less efficient compared to lead. On the other hand, wood is inexpensive and requires simple methods to fabricate; however, it is characterized by low density(Almond, 2002, Design, 2005).

Thus, concrete usually selected based on the aforementioned advantageous properties. However, concrete that contains cement accounts for approximately between 6% to 7% of all CO_2 emission in the atmosphere. In turn, CO_2 contributes

almost 65% of global warming (Rashad, 2014). In addition, building materials are the second main source of indoor radon pollution, after soil, with concrete among the highest contributors (Turhan et al., 2010, Folkerts et al., 1984). Moreover, the exhalation of radon and progenies from indoor concrete surfaces has been found to contribute up to 30% of the overall indoor radioactive pollution (Taylor-Lange et al., 2012).

Hence, efforts have been made to replace parts of the OPC with pozzolans. Recently, silicon and aluminum activated in alkali solution was recognized as a substitute for cementitious material (Davidovits, 1999a). FA, also referred to as geopolymer or alkali-activated FA, is typically used as a precursor to develop this cementitious material (Bakharev, 2005, Fernández-Jiménez et al., 2005). The mortar and concrete developed from this geopolymer display strength and form comparable to those formed with conventional OPC. In addition, geopolymers possess exceptional mechanical properties and resistance to acid and fire (Rattanasak et al., 2010) .

Geopolymers are inorganic cementitious binding gel developed from the polymerization of aluminosilica rich material with alkali metal hydroxide/silicate liquid, which can be used to encapsulate fine and coarse aggregates to produce concrete (Salwa et al., 2013, Davidovits, 1982, Davidovits, 1991, Davidovits, 1994c, Xu and Van Deventer, 2000). Davidovits (1994c) Stated that geopolymers have high early strength and improved durability and pose no health risk. The alternative form of cementitious materials using silicon and aluminum activated in a high alkali solution was established by (Davidovits, 1991). This geopolymer is usually made of FA activated with alkaline solution and sand(Rattanasak and Chindaprasirt, 2009).

Geopolymer paste is largely used as an alternative binder to OPC pastes in the production of concrete. Although FA is a source material for readily available geopolymer binders, its current use is limited. More specifically, although the worldwide coal ash production surpasses 390 million tons annually, its usage fell under 15% based on the report (Ranjbar et al., 2014). Therefore, efforts to exploit the use of FA as a binder in the manufacture of concrete are significant in order to make it more environmentally viable (Hardjito et al., 2004b). Barium sulfate ($BaSO_4$) base is the preferred material for shielding the effects of radiation (Akkurt et al., 2005, Kim et al., 2012b, Salah et al., 2009). However, $BaSO_4$ only produces a good shielding effect when it is a good spread over other materials because of its high density ($4.5 g/cm^3$).

This study will focus on waste material FAGP as an alternative to OPC in radiation shielding. The material is not expensive and not toxic (i.e. environmentally friendly), but its atomic number may be low and thus affect their effectiveness in shielding. Therefore, some elements have a high atomic number and good absorbing properties such as Barite with the chemical formula of $BaSO_4$. Moreover, this non-metallic crystalline material is 4-4.5 g/cm^3 dense (Mostofinejad et al., 2012). The thickness of the shielding material depends on the amount of radiations to be absorbed and the energy levels of the radioactive particles (Akkurt et al., 2012). This study measures the atomic number and μ/ρ of FAGP. $BaSO_4$ will be added as additional material to increase the atomic number of FAGP. To know the ability of FAGP in attenuating the radiation, mass and linear attenuation coefficient will be the calculated for the FAGP and (FAGP with different percentages of $BaSO_4$). To determine the thickness of the FAGP which is sufficient for a certain thickness of lead in the attenuation of radiation at different energies of the diagnostic radiation,

different thicknesses for the FAGP will be compared with different thicknesses of the lead in X-ray attenuation.

1.2 Problem statement

The radiation workers are subjected to radiation exposure in laboratories and hospitals. In this manner, their lives are prone to future risks, which may include some serious diseases. Taking, this into account, there is a need for using shielding materials that can reduce radiation risks. Thus, researchers have been very concerned about finding ways to solve this critical problem. They used various materials for shielding such as lead, concrete and OPC to minimize the radiation risks. However, it has been, reported that these materials have some shortcomings such as high cost and toxicity.

Researchers attention has been directed toward the high cost and toxicity of lead (Scuderi et al., 2006). Such given attention has highlighted that the toxicity of lead is a major concern because it is a heavy metal that can produce a range of radiation permitted for an occupational exposure and in vivo absorption during the work (Kim and Park, 2011). Consequently, there are various problems related to the use of lead as a shielding material in a clinical setting (Kim et al., 2003).

Concrete also used as a radiation shielding material. However, it has been reported that concrete is expensive, with some problems that are related to inconsistency in its composition and its moisture content. Furthermore, while water content lowers both the density and structural strength of concrete, the disparity in its composition brings about ambiguity in calculations that are done for shield design predictions of the radiation distribution and attenuation (Manohara et al., 2009).

Although OPC has been used as a radiation shielding material, its production burns large quantities of CO_2 emissions (Kong and Sanjayan, 2008). This confirms that using OPC in shielding produces a large amount of CO_2, which in turn can increase environmental pollution. Considering the problems related to the use of lead, concrete and OPC as shielding materials.

Therefore, the problems mentioned in the lead and concrete materials previously used in shielding are given concern in this study to use FAGP as an alternative material for OPC in shielding. In this study, geopolymer was fabricated from FA, which is a solid residue derived from coal burning thermal power stations. This study suggested that FA might be activated using alkaline liquids to form FAGP to replace the use of OPC in concrete. FAGP is an environmentally friendly material as it does not emit greenhouse gases during the polymerization process and it is also non-toxic material (Hardjito and Rangan, 2005). Moreover, the technology of geopolymer has been reported to have the potential to decrease CO_2 emissions by 80% (Davidovits, 1994a). Notwithstanding, efforts to use FA in concrete manufacture are important to make concrete more environmentally friendly (Hardjito et al., 2004a). There are four main concerns to use FAGP as a shielding material in this study.

First, the materials used in shielding require having a high effective atomic number, which makes the shielding material able to attenuate the radiation that passes through the shielding materials. This current work examines the possibility of using FAGP as an alternative material to replace OPC in the shielding of radiation. Specifically, this study highlights that the use of FAGP in the shielding requires studying effective atomic number (Z_{eff}) and adding some additional material with a

high (Z_{eff}) value material such as $BaSO_4$. These two processes are carried, out to improve FAGP for shielding.

Secondly, the μ and μ/ρ are important parameters in understanding the ability of the FAGP used in radiation shielding. Therefore, this study focuses on the measurement of the μ and μ/ρ of the FAGP and OPC samples in order to recognize the ability of these materials in attenuating radiation.

Thirdly, the addition of materials that has a high Z_{eff} such as $BaSO_4$ to FAGP for shielding increases the ability of the material to attenuation, and therefore, must be added at different and limited percentages, so that it does not affect the proportion of the main material (FAGP). This is followed by choosing the optimum value to compare the attenuation of the FAGP with lead. Therefore, it is necessary that this study must focus on the determination of the optimum value of the $BaSO_4$ that was added to the FAGP in order to obtain the ability of attenuation of FAGP to lead.

Four, the determination of success in used FAGP for shielding in this study, the best results obtained from this study regarding both the thickness and the added ratio of $BaSO_4$ after determining the Z_{eff}, should be applied in the fabrication of a small shielding box to be used in the laboratory for the point sources. The evaluation of the performance of this shielding box is carried out by the use of diagnostic X-ray on different energies.

1.3 Objectives of the study

The overall aim of this study is to use FAGP as an alternative material for OPC in shielding by enhancing the properties of FAGP by adding $BaSO_4$ to protecting against of diagnostic radiology. The objectives of this study are:

i. To fabricate the FAGP samples with 5, 10 and 15% of $BaSO_4$, prepare the OPC and determine the effective atomic number (Z_{eff}) for the FAGP and OPC samples using EDX analysis.

ii. To measure the μ and μ/ρ of the FAGP and OPC samples using XCOM software, XRF and narrow beam geometry.

iii. To compare the FAGP + 15% $BaSO_4$ thicknesses with the thicknesses of lead and to obtaining the thickness of FAGP that is equivalent to the 1mm thickness of lead using X-ray diagnostic with 80, 100, and 120 kV.

iv. To fabricate the FAGP shielding box from the optimum result of thickness and $BaSO_4$ percentage, and to evaluate the shielding box performance by diagnostic X-ray.

1.4 Scope of research

In this study, the FAGP will use as a shielding material used for radiation protection. The FA will be a resolved in alkaline solution and the $BaSO_4$ will add to the FAGP by 5, 10 and 15 % percentages. Z_{eff} for all the samples will be calculated by EDX measurements. XCOM, XRF and narrow beam geometry will be used to measure the μ and μ/ρ for all the samples. In addition, the attenuation coefficients will be evaluated utilizing X-ray with different thicknesses of lead and FAGP to detect the equivalent thicknesses for lead and FAGP. The effectiveness of design shielding box will be evaluated utilizing ion chamber and Gafchromic XR-QA2 films dosimeters.

1.5 Structure of thesis

This thesis comprises of five chapters. Chapter 1 introduces shielding protection, shielding materials and history of the FAGP. The problem statement,

research objectives and scope of research are also dealt with in chapter one. Chapter 2 presents a comprehensive review of theoretical background and literature review with strengths and limitations of the field of study. Chapter 3 presents a detailed synopsis of research methodology comprising the experimental procedures of OPC and FAGP. The $BaSO_4$ added to the FAGP to enhance its properties. (The equipment used in this study also dealt with in this chapter). The design-shielding box explained in details fabrication and evaluation performance. Chapter 4 covers the results and discussion of all the experiments performed in this study comprise the percentages of elements in the components, the μ/ρ studied by narrow beam and XRF, the thicknesses of FAGP have been studied by comparing to the equivalent of lead thickness for X-ray diagnostic using different energies. This chapter ended with fabricating the shielding box from the optimum parameters then followed by evaluating the design shielding box performance for X-ray diagnostic. Finally, chapter 5 presents the major findings of the study and provides suggestions and recommendations for future research.

CHAPTER 2: THEORETICAL BACKGROUND AND LITERATURE REVIEW

2.1 Introduction

This chapter provides a detailed description and concise review of theories and concepts that are deemed relevant to the subject area of this study. This chapter starts with an account of the X-ray equipment (X-ray tube characteristics of X-ray Spectrum and Bremsstrahlung X-rays). Photon interactions with the matter, photoelectric effect, coherent scattering, Compton scattering and pair production are also addressed in this chapter. This is followed by the description of photon beam attenuation (μ and μ/ρ). X-ray production, XRF, radiochromic film, the biological effect of radiation and radiation protection factors are also explicated in this chapter. To the end of this chapter, there is a review of radiation shielding materials such as lead, concrete, OPC and FAGP (with $BaSO_4$ as an additive).

2.2 X-ray tubes

The most conventional system that is used for producing X-rays is the X-ray tube which is given in Figure 2.1. This X-ray tube comprises a totally evacuated glass envelope, which consists of a cathode and an anode. The cathode contains a filament. The production of electrons takes place as a result of the application of electrical current by the filament in the cathode. These electrons interact with the anode, which contains the essential spot involved in X-ray production, on the second side of the X-ray tube (Fosbinder and Orth, 2011).

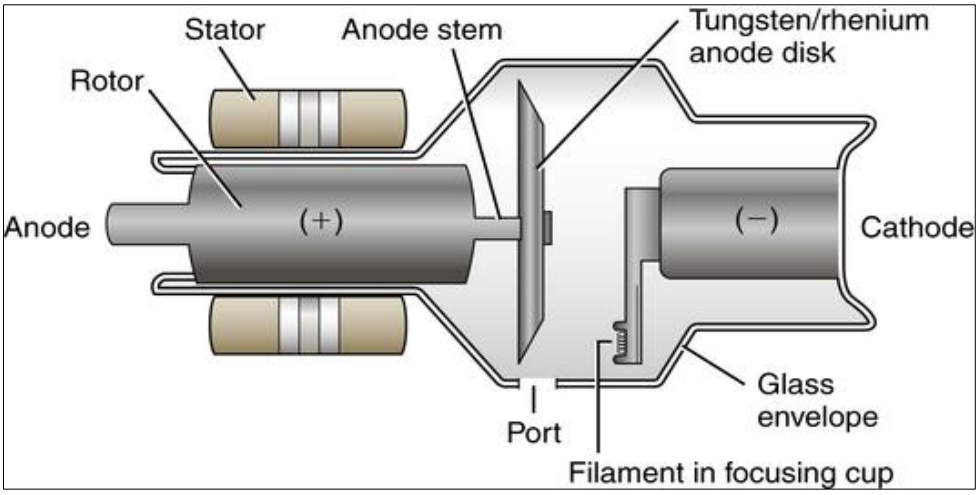

Figure 2.1 Components of a typical X-ray tube (Fosbinder and Orth, 2011)

2.2.1 Characteristics of X-ray spectrum

Various X-ray energies are specified by the energy spectrum. The typical X-ray is dependent on Z_{eff} of the target atom (Bushberg and Boone, 2011). Thus, the peaks of the discrete energy spectrum produced by the characteristic X-rays are distinctly defined energies that are related to the disparity between the atomic energy levels of the anode atoms involved in the electronic transitions (Fosbinder and Orth, 2011). In addition, X-ray spectrum is also identified by a continuous curve that is associated with the Bremsstrahlung radiation phenomenon (Seibert and Boone, 2005). Hence, the emitted X-ray spectrum is a blend of the distinctive spectral peaks of a specific anode material and the Bremsstrahlung radiation that exists in all X-ray tubes. The maximum photon energy (kVp) is derived from the voltage applied to the tube known. The peak of the X-ray spectrum is approximately half of the maximum energy (Seibert and Boone, 2005). As shown in Figure 2.2, filters are usually placed in front of the exit window to remove low energy X-rays that do not add to the ultimate image.

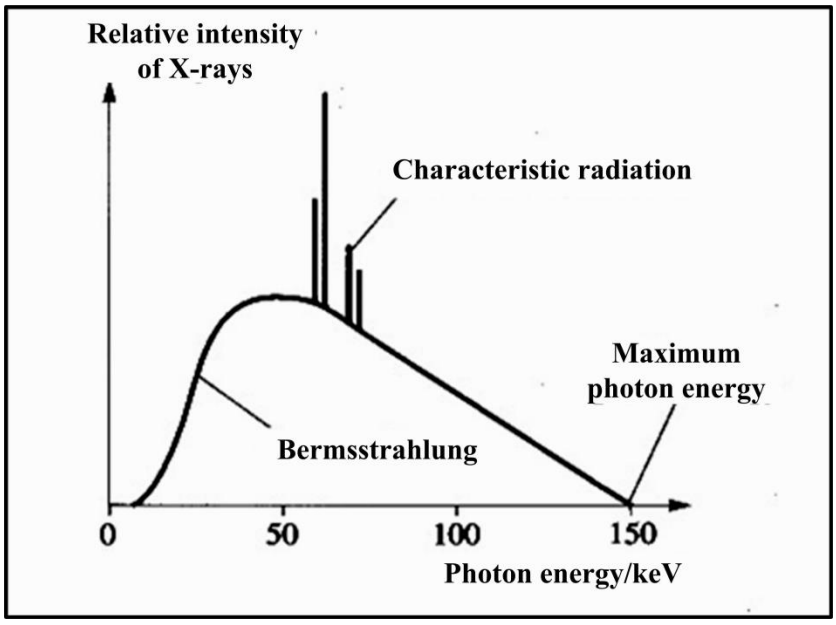

Figure 2.2 Beam output spectrum for X-ray tube (Fosbinder and Orth, 2011)

The interactions between electrons occur in the inner shell (e.g. K-shell electrons) of the target atom. The kinetic energy of the incident electron surpasses the binding energy of inner shell electron resulting in expulsion of the bound electron. As a result of this expulsion of the bound electron, a vacancy that puts the atom in an unstable state is created. To regain stability, an electron from the succeeding level will attempt to fill this vacancy. This transition is followed by an emission of electromagnetic radiation in form of X-rays, which are also referred to as characteristic X-rays. These X-rays are denoted as characteristic X-rays because such intricate interaction between electrons is characteristic of the element involved**.** The X-rays emitted when an electron drops from L-shell to K-shell and from M-shell to K-shell are referred to as K-alpha and K-beta X-rays, respectively. Although it is possible for M-L transitions and others to occur, this possibility is so low that they can be soundly disregarded. Each element has its characteristic nuclear binding

energies and distinctive radiation that is dependent on the binding energy of a specific element (Johns, 1983).

2.2.2 Bremsstrahlung X-rays

Bremsstrahlung is the process that involves the interaction between the accelerated electrons and the electrostatic force field of the nucleus. In the bremsstrahlung process, the columbic force of attraction initiates the deceleration and deviation of an electron from its original path. As a result of this, a portion or the entire of its energy is emitted as electromagnetic radiation, i.e. an X-ray photon.

Given that the electron has the probability of having one or more bremsstrahlung interactions with the target material, the resultant bremsstrahlung photon may have energy equal to the original energy of the electron. Therefore, the appearance of bremsstrahlung radiation is a continuous portion in the X-ray spectrum (Ball et al., 1997). The probability of bremsstrahlung production is directly proportional to Z^2 of target material. The bremsstrahlung interaction is more likely to occur with increased density of the atom. However, the first power of atomic number and the voltage applied to the x-ray tube determine the efficiency of X-ray production. This efficiency is defined as the ratio of output energy emitted as X-rays to the input energy deposited by electrons. Figure 2.3 as given below to illustrate this and to show projectile electron producing bremsstrahlung X-rays of different energies. As shown in Figure 2.3, the efficiency of X-ray production with tungsten target for electrons accelerated through 100 V is below 1%, whereas 99% of kinetic energy of the electrons is converted to heat.

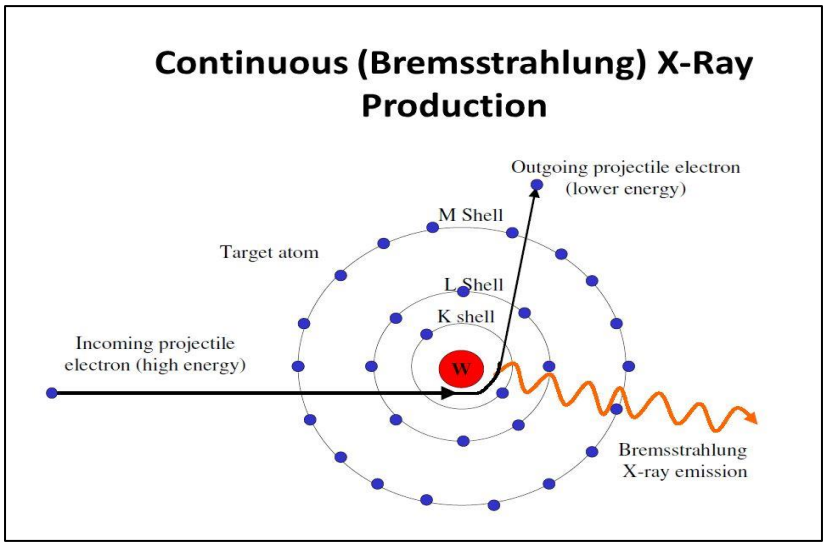

Figure 2.3 Projectile electron producing bremsstrahlung X-rays of different energies (Fosbinder and Orth, 2011)

2.3 Production of X-rays

Since its discovery, X-rays have been extensively employed in diagnostic radiology. X-rays are produced by interactions in atomic shells. Conventionally, X-ray photons are generated via the emission of electrons from a filament (cathode), which are then accelerated with a voltage toward a target (anode). Afterwards, the electrons strike the target, thus converting a small fraction of their kinetic energy into X-ray photons. These interactions between a target element and electrons produce rays with different spectra depending on specific elements. In this process, an X-ray device emits bremsstrahlung and characteristic X-ray photons through some physical mechanisms (Van Grieken and Markowicz, 2001).

2.4 Photon interactions with matter

This section deals with the explanation of the photon interaction with matter. As X-ray or γ-ray beam travels through a matter, it is subjected to transmission, scattering, or absorption. The X-rays or γ-rays transfer their energy to a matter through interactions with electrons and atomic nuclei. The interception of these high energy rays by an atom results in the ejection of electrons from the atom or the excitation of electrons. However, the behaviour of photons in the matter is completely different from that of charged particles because photons do not possess an electric charge, which makes the numerous inelastic collisions with atomic electrons impossible. For this type of radiation, the most significant mechanisms of interaction include photoelectric effect, Compton scattering, coherent scattering, and pair production (Kurudirek and Topcuoglu, 2011). These mechanisms are described in the following sub-sections.

2.4.1 The photoelectric effect

The photoelectric effect or interaction involves the complete absorption of incident photon by the atom. The photon energy is entirely transmitted to an inner-shell electron. The atom then undergoes ionization when this electron is expelled from the atom. The ejected electron is referred to as photoelectron. The kinetic energy of photoelectron is equal to the difference between the incident photon and the binding energy of the inner-shell electron. This is presented mathematically in Equation (2.1):

$$E_i = E_b + E_{ke} \tag{2.1}$$

where, E_i denotes the energy of the incident photon, E_b represents the binding energy of the electron, and E_{ke} signifies the kinetic energy of the photoelectron. To

ensure photoelectric interaction, the incident photon requires an energy that marginally exceeds the binding energy of the electron. The majority of atoms in tissue have very low atomic number elements and very low K-shell binding energies. The photoelectron is composed of matter and it travels < 1 mm in tissue. This type of confined absorption produces biological changes. The removal of electron of the atom causes instability of the atom. The vacancy in the K shell becomes filled with an electron from the L shell, M shell, or a free electron. Filling the inner-shell vacancy generates typical or characteristic X-ray photons. Characteristic photons from tissue elements (carbon, nitrogen, and oxygen) are typified by very low energies. They are referred to as secondary radiation and behave like scatter radiation. As shown in Figure 2.4 above, the majority of characteristic X-rays from the tissue do not leave the patient due to their exceptionally low energies. Thus, there is no exit radiation after a photoelectric interaction. In addition, the photoelectric effect, which is the source of lighter densities observed on conventional X-ray images, causes complete absorption of the incident photon.

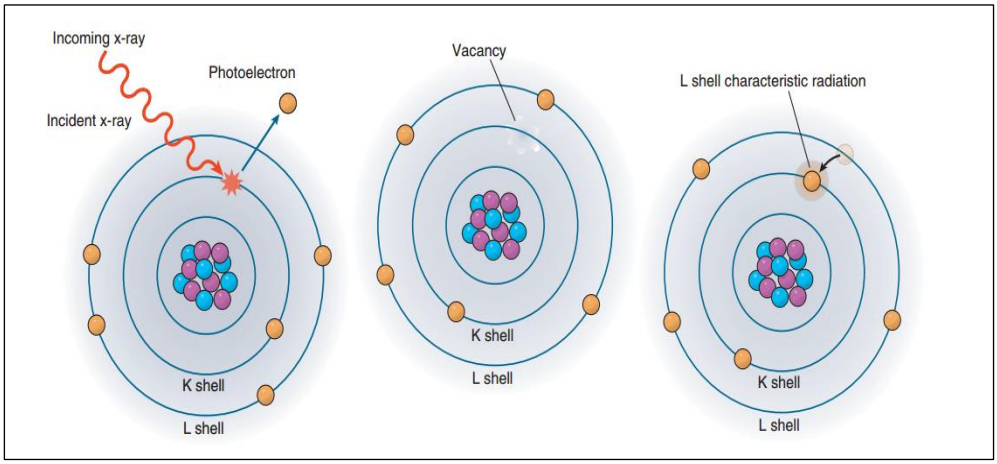

Figure 2.4 Photoelectric effect phenomenon (Fosbinder and Orth, 2011)

When the atomic number (Z) concomitantly increases, the photoelectric effect increases. Higher X-ray photons absorption occurs in atoms with higher atomic numbers. Compared to muscles, bones generally display higher photons absorption due to their higher atomic number. The X-ray attenuation of a bone is four times greater than that of muscle at X-ray energy of 40 keV. Barium and iodine are used as contrast agents to increase photoelectric effect due to their high atomic numbers. Structures encompassing these radiopaque contrast agents appear lighter or brighter on conventional radiographic images. Another known fact is that photoelectric effect decreases as X-ray energy increases. The proportionality of this interaction is mathematically illustrated in Equation 2.2.

$$\tau \; \alpha \; Z^n (h\gamma)^{-3} \qquad (2.2)$$

where (τ) symbolizes the probability of the photoelectric effect, Z denotes the atomic number of the bombarded mater, n is 3 or 4 depending on the energy of the photon, and (h γ) represents the energy of the primary photon (Saha, 2012).

2.4.2 Coherent scattering

Coherent scattering, also referred to as classical scattering, arises from incident photon interaction with electrons in an atom, resulting in excitation and vibration of the electrons. The excited atom instantaneously expels the excess energy as a scattered X-ray photon with the same wavelength as the incident photon, as shown in Figure 2.5.

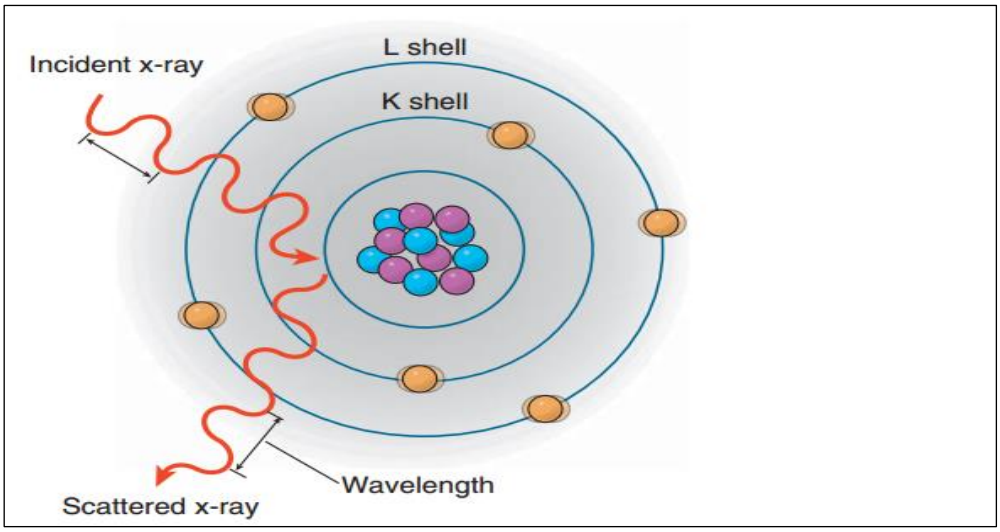

Figure 2.5 Coherent scattering (Fosbinder and Orth, 2011)

With reference to Figure 2.5, Coherent scattering has been defined as Thompson or classical elastic scatter that modifies the direction of X-ray photon with no variation in energy (Attix, 2008). It occurs principally at energies below 10 keV and is an insignificant phenomenon in diagnostic radiology.

2.4.3 Compton scattering

Compton scattering involves the interaction between the incident X-ray photon and a loosely bound outer-shell electron .the ionization of the atom done by incident X-ray photon causes the removal of an outer-shell electron and change the direction of the photon. The Compton scattered electron and the scattered X-ray photon share the incident photon energy. Compared to the incident photon, the Compton scattered X-ray photon is identified by its lower energy and longer wavelength Figure 2.6.

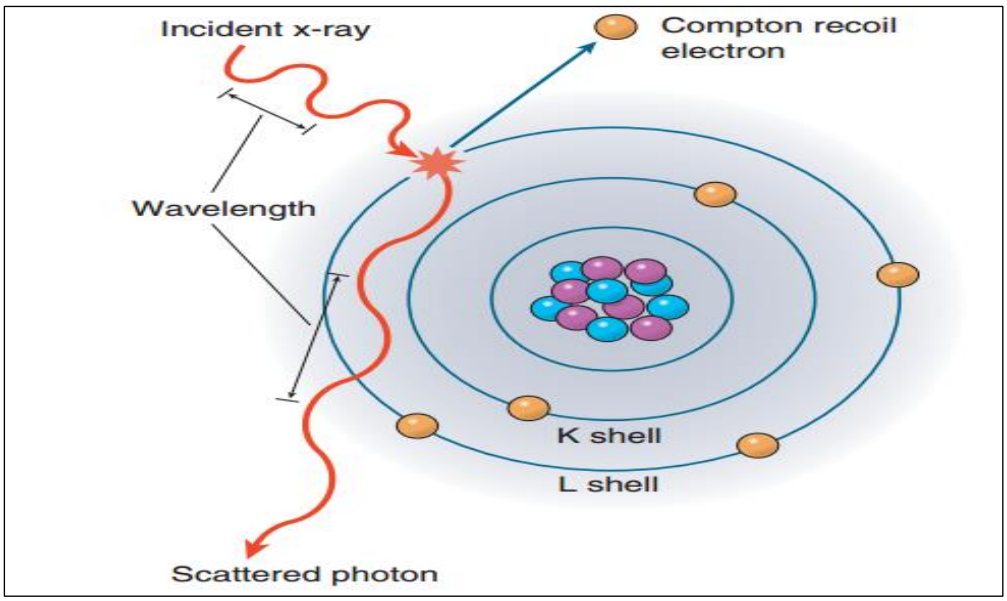

Figure 2.6 Compton scattering of an incident X-ray by an outer-shell electron (Fosbinder and Orth, 2011)

The Compton scattering is not affected by variations in material and atomic number. In research on radiography of larger organs of the body, it has been revealed that higher irradiation of tissues occurs as a result of the larger field sizes. This leads to initiating more Compton scattering. The scatter radiation emitted from the patient is the main source of occupational exposure for radiographers. Fluoroscopic examination is a severe radiation risk due to the enormous quantity of radiation that is scattered from the patient. Thus, it is essential for radiographers to wear radiation protection apparels such as lead apron, thyroid shield, and gloves throughout fluoroscopic analyses.

The volume of Compton scattering increases when X-ray energy increases. Compton scattered photons can be scattered in different directions at angles up to 180º. The deflection angle is dependent on the energy of the primary photon. At deflection angle of 0º, no energy is transferred because the path of the photon does not deviate from its original direction. When the deflection angle increases to 180º,

the energy specified for the recoil electron increases and less energy remains with the scattered photon. When a scattered photon is scattered back in the direction of the incident photon, it is referred to as backscatter radiation. As a result of backscatter radiation, the production of artefacts on the radiographic image may occur, reducing the quality of an image. The backscatter radiation drops excessive exposure on the image, which is termed radiation fog. It should be noted that when the radiation fog increases, the radiographic contrast decreases.

Nonetheless, only photoelectric and Compton interactions are significant phenomena in diagnostic radiology. At low energies, the Compton scattering and the photoelectric effect have approximately the same ratio of interactions, while Compton scattering is the dominant feature at higher energies shown in Figure 2.7.

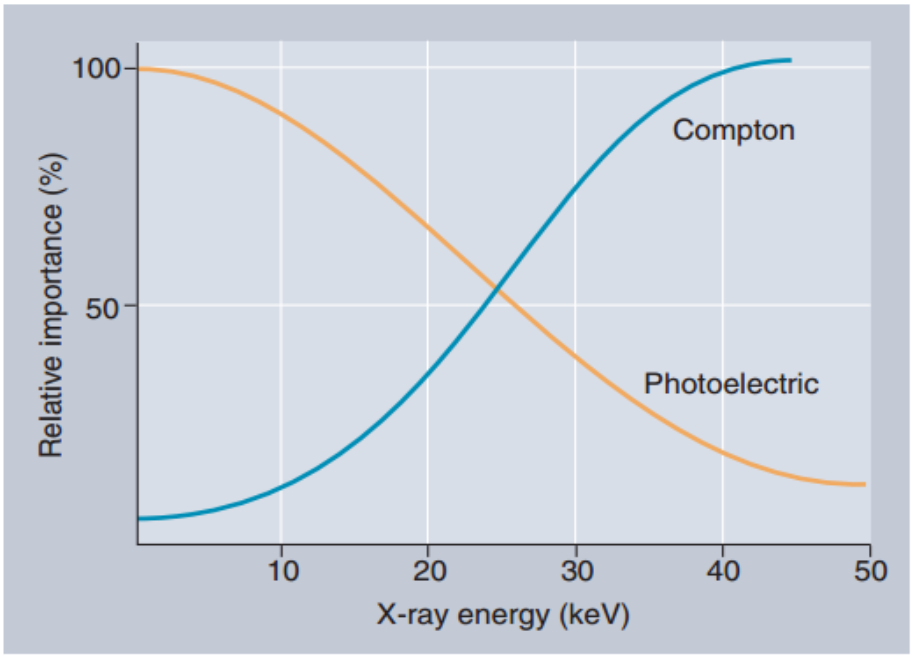

Figure 2.7 Demonstrates the relative importance of the photoelectric and Compton interactions as a function of X-ray energy (Fosbinder and Orth, 2011)

As reflected in Figure 2.7 when the incident X-ray photon energy increases, the relative amount of photoelectric interaction decrease and relative amount of Compton scattering increases.

2.5 Photon beam attenuation

The interaction between incident X-ray photon beam and absorber material of a specified thickness results in attenuation of the photon beam via absorption or scattering. Attenuation is the gradual decline in the intensity of photon beam of any kind of flux through a medium. Attenuation coefficient is a parameter that defines the ease by which a beam of photons can penetrate a material. Large attenuation coefficient suggests the intensity of the incident beam rapidly declines as it travels through a medium, while small attenuation coefficient shows that the material is relatively transparent to the incident photon beam (Attix, 2008). Attenuation coefficient is explained further in the following subsection.

2.5.1 Linear attenuation coefficient

As a beam of monenergistic photons travels through a material, its intensity decreases due to interactions between the beam and the material, which results in exponential attenuation. The exponential attenuation of beam intensity is determined primarily by thickness, density, and atomic number of the material. Figure 2.8 conceptualizes linear attenuation coefficient (Radiation, ARPANSA) based on the penetration and intensity reduction of the incident photons beam through a material.

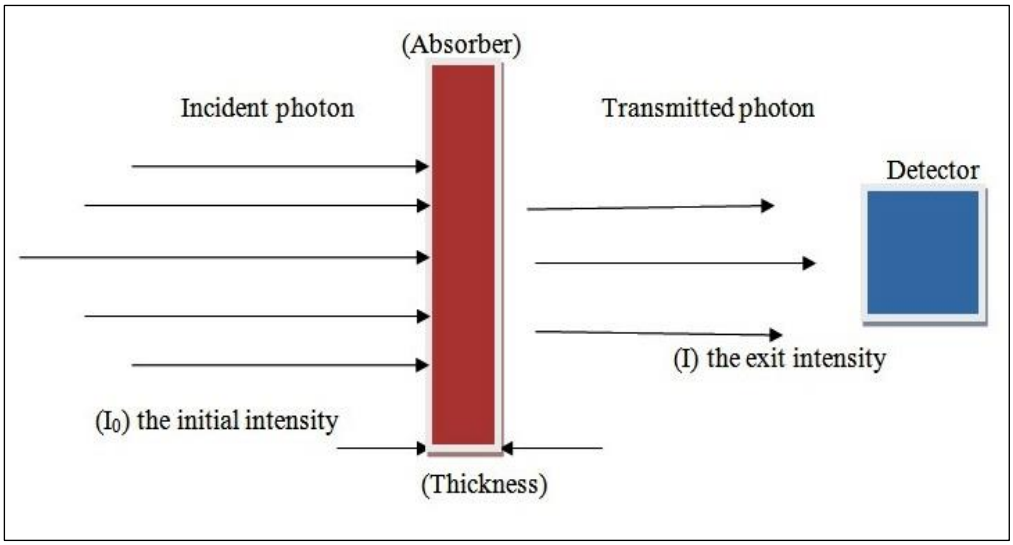

Figure 2.8 Attenuation and transmission of X-ray though absorber

The initial intensity of incident beam is denoted as I_0, the beam intensity at the exit point of the thickness is symbolized by I, and the exponential function of the material thickness is expressed as x (cm). The intensity of the beam generally decreases exponentially when the thickness of the absorber increases. As the exponential function of the material thickness; μ is typically measured in cm^{-1}, thus μ can be calculated, as shown in Equation 2.3.

$$\frac{I}{I_o} = e^{-\mu x} \tag{2.3}$$

where μ increases linearly with material density ρ; thus, dense materials display relatively higher attenuations. Generally, μ is affected by photon energy, atomic number (Z), and material thickness. Attenuation increases with lower photon energy, higher Z or thicker material (Powsner et al., 2013). In addition, the linear attenuation coefficient is the sum of individual (μ) of each material type due to the different types of photon beam interactions.